JOURNAL OF Materials CHEMISTRY

Crystal structure and thermal behaviour of the new layered oxalate $Y(H_2O)Cs(C_2O_4)_2$ studied by powder X-ray diffraction

Thierry Bataille, Jean-Paul Auffrédic and Daniel Louër*

Laboratoire de Chimie du Solide et Inorganique Moléculaire, UMR CNRS 6511, Université de Rennes, Avenue du Général Leclerc, 35042 Rennes cedex, France.
E-mail: Daniel.Louer@univ-rennes1.fr

Received 14th February 2000, Accepted 14th April 2000
Published on the Web 5th June 2000

The crystal structure of the new mixed oxalate $Y(H_2O)Cs(C_2O_4)_2$ has been solved from powder X-ray diffraction data. The compound is isostructural with the related yttrium ammonium oxalate. It crystallises with monoclinic symmetry, $a=8.979(2)$, $b=6.2299(8)$, $c=8.103(1)$ Å, $\beta=90.05(2)^\circ$ and $V=453.3$ Å^3, in space group $P2/n$. Its layered structure consists of corrugated planes of yttrium atoms linked by the oxalate groups, between which are intercalated the caesium atoms. The water molecule is connected to the yttrium atom and lies in the interlayer spacing. The thermal behaviour of the title compound has been characterised by means of temperature dependent X-ray diffraction (TDXD) and thermal analyses. Anhydrous yttrium caesium oxalate has been observed and isolated. Thermal decomposition of the mixed oxalate provides a new high-temperature orthorhombic modification of Cs_2CO_3.

Introduction

Mixed oxalates derived from rare earths (and yttrium) and monovalent cations, with the general formula $LnM^I(C_2O_4)_2{\cdot}nH_2O$, have been the subject of many investigations.[1–6] For some of them, interesting 'dynamic' properties have been reported recently. Indeed, the rôle of zeolitic water molecules in $YK(C_2O_4)_2{\cdot}4H_2O$ has been demonstrated from powder diffraction data[7] and cation exchange properties have been described for $La(H_2O)_2NH_4(C_2O_4)_2{\cdot}H_2O$.[8] In the latter case, the exchange of ammonium groups by U(IV) and Th has been reported and an application in nuclear technology for enrichment processes in nuclear wastes has been suggested.[8] These phases have been synthesised in a powder form, hence, it is mainly from X-ray powder diffraction data that their crystal structures have been elucidated. The crystal structure determinations have shed light on the crystal chemistry and dependent properties of these oxalate materials. Two structure types have been identified for these compounds: a three-dimensional structure exhibiting tunnels with square and ellipsoidal cross-sections is observed for the yttrium potassium phase,[7] while a two-dimensional structure has been reported for $La(H_2O)_2M(C_2O_4)_2{\cdot}H_2O$ (M = K, NH_4).[9] This layered-type structure with a monovalent cation located between the layers helps to explain the ion exchange properties of these phases. The present study deals with the extension of the series to the new yttrium caesium oxalate phase. The synthesis of this compound is described, as well as the crystal structure determination, carried out using powder diffraction data collected with a conventional X-ray source, and the thermal behaviour, carefully investigated by thermal analytical methods, including temperature dependent X-ray diffraction.

Synthesis

The method described by Barrett *et al.*[2] for the synthesis of double oxalates of ammonium and rare earth or yttrium elements was used initially, but a mixture of the two phases $Y(H_2O)Cs(C_2O_4)_2$ and $Y_2(C_2O_4)_3{\cdot}10H_2O$ was obtained. Consequently, pure $Y(H_2O)Cs(C_2O_4)_2$ was obtained as follows: 15 ml of an aqueous solution of $Y(NO_3)_3{\cdot}5H_2O$ (0.25 mol l^{-1}) was added dropwise to 20 ml of a solution of $Cs_2C_2O_4$ (0.5 mol l^{-1}). The precipitate was filtered off and dried at room temperature. The Y : Cs ratio (1 : 1) was confirmed by energy dispersive spectrometry (EDS) and the chemical formula from the crystal structure determination and thermogravimetric (TG) analyses. Anhydrous yttrium caesium oxalate was obtained from the precursor heated under a nitrogen stream at 190 °C for a few hours.

Experimental

Collection of powder X-ray diffraction data

X-Ray powder diffraction data for $Y(H_2O)Cs(C_2O_4)_2$ were collected with a Siemens D500 high-resolution powder diffractometer using the focusing Bragg–Brentano geometry and monochromatic X-rays [λ(Cu-Kα_1) = 1.5406 Å]. The characteristics of the diffractometer have been described elsewhere.[10] The powdered sample was mounted in a top-loaded sample holder.[11] The pattern was scanned over the angular range 10–130° (2θ), with a step size of 0.02° (2θ) and times of 30 s step^{-1} to 70° (2θ) and 60 s step^{-1} from 70.02° (2θ) to the end of the scan. Then the full pattern was scaled to the lower counting time.

High-temperature powder diffraction data were collected *in situ* with a Bruker D5005 diffractometer, using Cu-Kα radiation [λ(Kα_1) = 1.5406, λ(Kα_2) = 1.5444 Å] selected with a diffracted-beam graphite monochromator, equipped with an Anton Paar HTK1200 high-temperature oven-camera. The pattern of $YCs(C_2O_4)_2$ was scanned over the angular range 10–90° (2θ) with a step size of 0.02° (2θ) and 100 s step^{-1}.

For pattern indexing, the extraction of peak positions was carried out by means of the Socabim program PROFILE, which is a part of the DIFFRAC-AT package supplied by Bruker AXS. Pattern indexing was carried out with the program DICVOL91.[12] Rietveld refinements were performed with the program FULLPROF99,[13] available in the package WINPLOTR.[14] Structure drawings were carried out with DIAMOND 2.1c, supplied by Crystal Impact, Bonn, Germany.

DOI: 10.1039/b001201g

Thermal analyses

Temperature dependent X-ray diffraction (TDXD) was carried out with a powder diffractometer (Cu-Kα_1 radiation) combining a curved position-sensitive detector from INEL (CPS 120) and a high-temperature attachment from Rigaku. An angle of 6° was selected between the incident beam and the surface of the stationary sample. The thermal decomposition of $Y(H_2O)Cs(C_2O_4)_2$ was carried out under flowing nitrogen with a heating rate of 5 °C h^{-1} up to 500 °C (counting time of 75 min per pattern) followed by a sudden decrease to room temperature. Thermogravimetric (TG) analysis was carried out with a Rigaku thermoflex instrument under similar experimental conditions.

Results

Structure determination of $Y(H_2O)Cs(C_2O_4)_2$

Pattern indexing. The indexing of the powder diffraction pattern from the first 20 lines led to an orthorhombic solution, with the unit cell parameters $a=8.977(2)$, $b=6.2300(9)$, $c=8.103(1)$ Å and $V=453.2$ Å^3 [$M_{20}=63$ and $F_{20}=108(0.007,28)$]. A monoclinic solution was also obtained with a similar set of unit cell parameters, *i.e.* $a=8.979(2)$, $b=6.2299(8)$, $c=8.103(1)$ Å, $\beta=90.05(2)°$ and $V=453.3$ Å^3 [$M_{20}=67$ and $F_{20}=108(0.005,39)$]. This latter solution was not initially retained, since the magnitude of the deviation from the orthorhombic cell was within the experimental errors for the observed data. Nevertheless, attempts to solve the structure with the orthorhombic symmetry were unsuccessful. Consequently, on the basis of similarities with the cell parameters of the related ammonium phase, $Y(H_2O)NH_4(C_2O_4)_2$ ($a=9.18\pm0.01$, $b=6.09\pm0.01$, $c=7.89\pm0.01$ Å, $\beta=90.2\pm0.1°$, $V=441.10$ Å^3),[3] the monoclinic solution was considered in the structure analysis described in the present study. The conditions for non-extinction were consistent with the space group $P2/n$. The powder data have been submitted to the ICDD for possible inclusion in the powder diffraction file.[15]

Structure solution. A least-squares Rietveld refinement using the program FULLPROF99 was carried out in the angular range 10–130° (2θ) containing 772 reflections, on the basis of the atomic positions given for $Y(H_2O)NH_4(C_2O_4)_2$.[3] An examination of the pattern revealed an anisotropic diffraction line broadening characterised by reflections hkl with $h=l$ narrower than the other diffraction lines. This observation was used in the Rietveld refinement by using two functions to describe the angular dependence of the peak width and shape. The pseudo-Voigt function was selected to define the broadened reflections with a possible variation of the mixing factor η and the Pearson VII function was used for the other lines ($m=2$). The refinement involved the following parameters: 28 atomic parameters (including 7 isotropic atomic displacement parameters), 1 scale factor, 1 zero-point, 4 cell parameters, 6 half-width parameters, 2 variables for the angular variation of η, 1 preferred orientation parameter and 5 coefficients used to describe the functional dependence of the background. Line asymmetry at low angles was modelled with the procedure introduced by Bérar and Baldinozzi,[16] in which there are four independent parameters. The refinement converged to satisfactory residual factors, $R_F=0.045$ and $R_{wp}=0.107$. Crystallographic data and details of the Rietveld refinement are given in Table 1. Fig. 1 shows the best agreement obtained between calculated and observed patterns. Final atomic position parameters are given in Table 2 and selected distances and angles are given in Table 3.

Table 1 Crystallographic data and details of the Rietveld refinement for $Y(H_2O)Cs(C_2O_4)_2$[a]

Z	2
Wavelength/Å	1.5406
2θ range/°	10–130
No. of atoms	9
No. of reflections	772
No. of structural parameters	29
No. of profile parameters	27
R_F	0.045
R_B	0.067
R_p	0.081
R_{wp}	0.107
R_{exp}	0.096

[a]For the definitions of the R factors, see ref. 17.

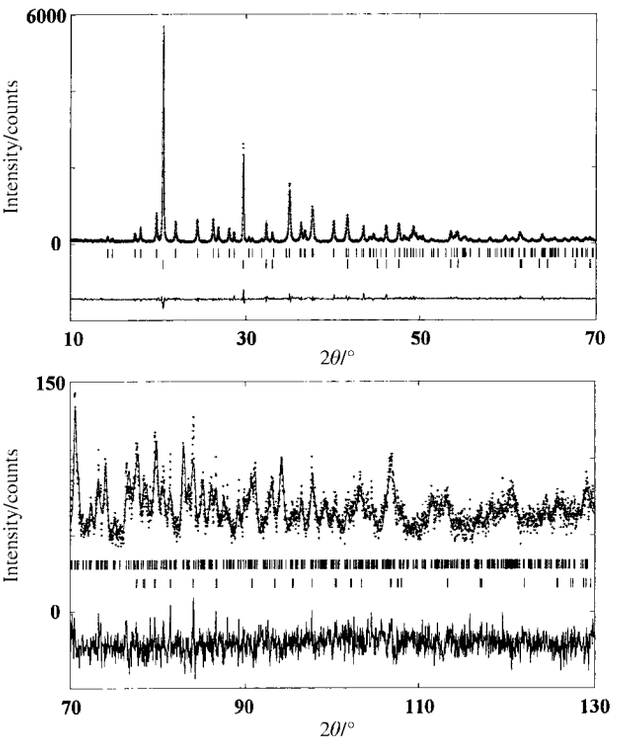

Fig. 1 Final Rietveld plot for $Y(H_2O)Cs(C_2O_4)_2$. Experimental data: dots; calculated pattern: solid line. The Bragg reflections are indicated by the vertical bars, the lower bars correspond to the hkh reflections modelled separately in the Rietveld refinement. The lower trace corresponds to the difference curve between observed and calculated patterns. Note that the intensity is magnified by a factor of 40 for the high-angle section.

Table 2 Fractional atomic coordinates and isotropic atomic displacement parameters for $Y(H_2O)Cs(C_2O_4)_2$

Atom	x	y	z	B_{iso}/Å^{2a}
Y	3/4	0.1058(4)	3/4	1.19(7)
Cs	1/4	0.4927(3)	3/4	2.74(7)
O11	0.3264(8)	0.118(2)	0.482(1)	0.1(2)
O12	0.526(1)	0.241(1)	0.604(1)	0.1(2)
O21	0.440(1)	0.160(2)	0.172(1)	0.4(3)
O22	0.901(1)	0.237(2)	0.522(2)	0.4(3)
C1	0.4537(9)	0.090(2)	0.541(2)	1.3(6)
C2	0.510(2)	0.109(2)	0.044(2)	0.9(6)
Ow	1/4	0.491(2)	1/4	0.8(4)

[a]Isotropic atomic displacement parameters were refined to the same value for O11 and O12, and for O21 and O22.

Table 3 Bond distances/Å and angles/° for $Y(H_2O)Cs(C_2O_4)_2$

Y:	$O11^{I}$	2.44(1)			
	$O11^{II}$	2.44(1)	C1:	$C1^{II}$	1.55(2)
	O12	2.48(1)		O11	1.25(1)
	$O12^{III}$	2.48(1)		O12	1.26(2)
	$O21^{I}$	2.46(1)			
	$O21^{II}$	2.46(1)		O11–C1–$C1^{II}$	115(1)
	O22	2.44(1)		O12–C1–$C1^{II}$	116(2)
	$O22^{III}$	2.44(1)		O11–C1–O12	121(2)
	Ow^{IV}	2.51(1)			
			C2:	$C2^{VIII}$	1.54(2)
Cs:	O11	3.26(1)		O21	1.25(2)
	$O11^{V}$	3.26(1)		$O22^{IX}$	1.25(2)
	O12	3.16(1)			
	$O12^{V}$	3.16(1)		O21–C2–$C2^{VIII}$	124(2)
	$O21^{VI}$	3.58(1)		$O22^{IX}$–C2–$C2^{VIII}$	116(2)
	$O21^{VII}$	3.58(1)		O21–C2–$O22^{IX}$	121(2)
	$O22^{VI}$	3.09(1)			
	$O22^{VII}$	3.09(1)			

[a]Symmetry codes: I: $1/2+x$, $-y$, $1/2+z$; II: $1-x$, $-y$, $1-z$; III: $3/2-x$, y, $3/2-z$; IV: $1/2+x$, $1-y$, $1/2+z$; V: $1/2-x$, y, $3/2-z$; VI: $-1/2+x$, $1-y$, $1/2+z$; VII: $1-x$, $1-y$, $1-z$; VIII: $1-x$, $-y$, $-z$;.IX: $3/2-x$, y, $1/2-z$.

Description of the structure

$Y(H_2O)Cs(C_2O_4)_2$ is isostructural with $Y(H_2O)NH_4(C_2O_4)_2$,[3] whose layered-type structure was described recently.[6] This two-dimensional structure is related to that of $Y(H_2O)Na(C_2O_4)_2\cdot 3H_2O$[18] and $La(H_2O)_2M(C_2O_4)_2\cdot H_2O$ (M = K, NH_4).[9] Fig. 2 shows that the structure consists of corrugated layers $[Y(C_2O_4)_2^-]_\infty$, parallel to (010), between which are intercalated caesium atoms and water molecules (superimposed on the Cs atoms in the projection shown in Fig. 2). Fig. 3 shows that the Cs atoms lie in 'windows' with almost square cross-sections defined by the oxalate groups. The yttrium atoms are ninefold coordinated by eight oxalate oxygen atoms and one water molecule. As shown in Fig. 4(a, b) the coordination polyhedron can be described as either a distorted antiprism monocapped by the water oxygen atom, or a distorted tricapped trigonal prism, as also reported for the structure of $Y(H_2O)NH_4(C_2O_4)_2$.[3] The distances between Y and O from the oxalate groups fall into the range 2.44(1)–2.48(1) Å, while the bond length to the water molecule is a bit elongated, *i.e.* 2.51(1) Å. Such bond lengths are slightly longer than the theoretical value (2.426 Å) calculated by the bond valence method[19] for yttrium atoms coordinated by nine oxygen atoms, and than the values observed for similar compounds, *e.g.*, 2.341(4)–2.481(6) Å for $Y(H_2O)Na(C_2O_4)_2\cdot 3H_2O$ and 2.34(1)–2.41(1) Å for $Y(H_2O)NH_4(C_2O_4)_2$. In addition, it is worthwhile to note that the Y–Ow distance is greater than the other Y–O distances in $Y(H_2O)Cs(C_2O_4)_2$, while the contrary is observed in the structure of $Y(H_2O)NH_4(C_2O_4)_2$ [2.34(3) Å].

The caesium atom is eightfold coordinated by oxalate oxygen atoms only. Its coordination polyhedron is also conveniently described as a slightly distorted tetrahedron defined by the C atoms of the oxalate groups, as shown in Fig. 4(c). The Cs–O bond lengths are in the range 3.09(1)–3.58(1) Å, which compares well with the theoretical value calculated by the bond valence method[19] for eightfold coordinated caesium atoms, *i.e.* 3.186 Å.

The bond distances and angles within the oxalate groups (Table 3) agree well with the values commonly reported in the literature for C_2O_4. The oxalate groups Ox1 and Ox2 are almost planar, the deviations from the mean plane are 0.087 and 0.003 Å, respectively.

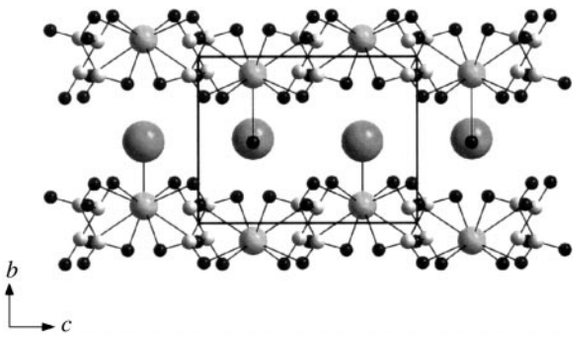

Fig. 2 Projection of the structure of $Y(H_2O)Cs(C_2O_4)_2$ along [100]. Cs: large grey spheres, Y: medium grey spheres, C: small grey spheres, O: small black spheres.

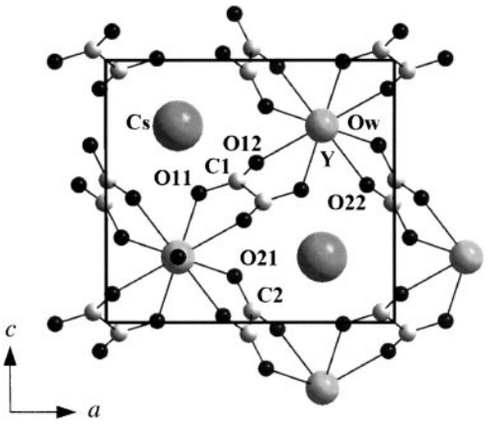

Fig. 3 Projection of the structure of $Y(H_2O)Cs(C_2O_4)_2$ along [010].

Thermal behaviour of $Y(H_2O)Cs(C_2O_4)_2$

Dehydration of the precursor. The TG curve in Fig. 5 shows that the dehydration of the precursor proceeds between room temperature and *ca.* 134 °C through two stages. An initial weight loss of 2.1% occurs gradually from room temperature to 107 °C, followed by a second rapid weight loss of 4.3% between 122 and 134 °C, from which a plateau is observed up to about 270 °C. The TDXD plot (Fig. 6) shows the successive powder diffraction patterns collected during the heating of the

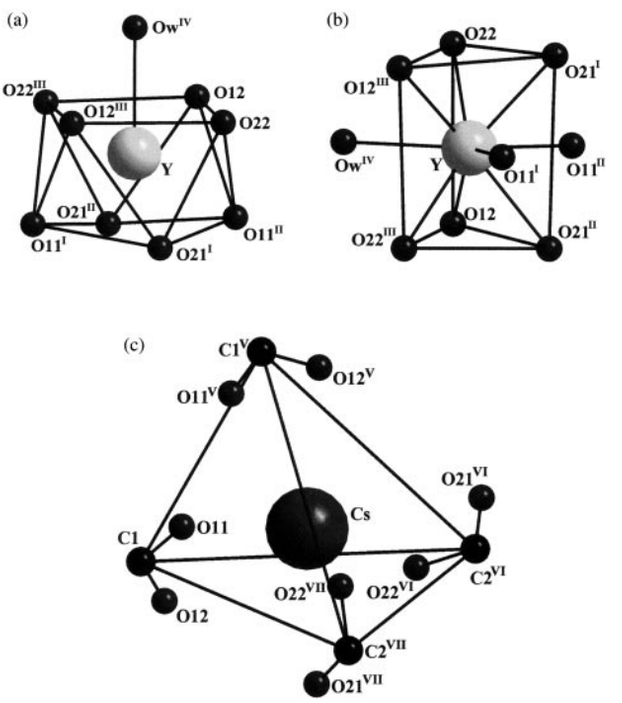

Fig. 4 Environment of the metal atoms. (a) Monocapped square-antiprism coordination around Y; (b) tricapped trigonal prism coordination around Y; (c) environment of Cs.

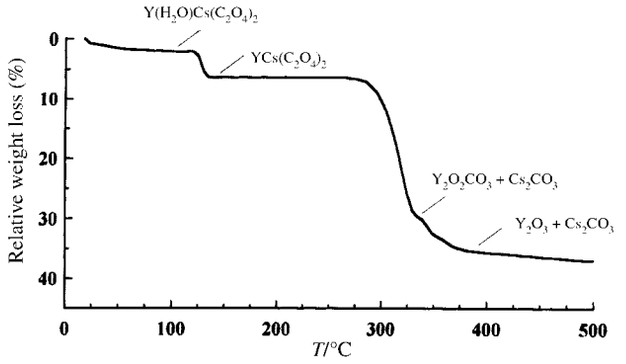

Fig. 5 TG curve for the decomposition of $Y(H_2O)Cs(C_2O_4)_2$ under flowing nitrogen (heating rate 5 °C h^{-1}).

precursor. No structural change occurs up to 115 °C and beyond this temperature the precursor transforms into a new phase identified as the anhydrous oxalate $YCs(C_2O_4)_2$, which is stable up to *ca.* 300 °C. The total weight loss of 6.4% observed at the plateau indicates that the water content in the precursor is 1.50 in ambient atmosphere at room temperature. From these observations it can be concluded that the first weight loss of 2.1% corresponds to the removal of 0.5 equivalents of H_2O adsorbed on the sample, and the second weight loss of 4.3% is due to the departure of the lone structurally bonded water molecule.

The powder diffraction pattern of the anhydrous oxalate, collected *in situ* at 190 °C, was indexed from the first 20 lines on the basis of a monoclinic solution, with $a=8.594(3)$, $b=6.236(1)$, $c=8.581(2)$ Å, $\beta=90.06(3)°$ and $V=459.90$ Å^3 [$M_{20}=28$ and $F_{20}=33(0.007,93)$]. This unit cell is found to be clearly similar to that obtained for the precursor. The conditions for non-extinction found were also consistent with the space group *P*2/*n*. The powder data have been submitted to the ICDD for possible inclusion in the powder diffraction file.[15] Only the yttrium and caesium atoms could be located by direct methods. They are located at positions similar to those obtained for $Y(H_2O)Cs(C_2O_4)_2$, *i.e.* 3/4, −0.0127, 3/4 for Y and 1/4, 0.5130, 3/4 for Cs. Although this result must be taken with caution, it would indicate that the structure of the anhydrous phase presents similarities to that of the precursor (see Table 2).

Decomposition of the anhydrous oxalate. The TG curve (Fig. 5) shows that $YCs(C_2O_4)_2$ loses weight rapidly between *ca.* 270 and 335 °C. At this temperature, an inflection is observed, where the weight loss of 29.5% is in agreement with the formation of a solid with the global composition '$YCsOCO_3$' (theoretical: 29.9%). The TDXD plot (Fig. 6) clearly shows the existence of a poorly crystalline phase in the temperature range 320–340 °C. The positions of the broad diffraction lines observed in the corresponding patterns were then assigned to the oxycarbonate $Y_2O_2CO_3$.[20] Consequently, in order to balance the mass change, it was necessary to suggest the simultaneous formation of Cs_2CO_3 in an amorphous state, since no additional diffraction lines were observed in these patterns. From 335 °C, the weight loss is slow and reaches 34.7% at *ca.* 370 °C, which is in agreement with the formation of a mixture of the two phases Y_2O_3 and Cs_2CO_3 (theoretical weight loss 35.1%). The formation of crystalline Y_2O_3 is clearly shown on the TDXD plot from 370 °C, but additional diffraction lines also emerge from the background. The latter do not arise from the Cs_2CO_3 phase known in the PDF2 data base.[15] Consequently, a high-temperature crystalline variant of Cs_2CO_3 can be suggested for the phase arising from the crystallisation of amorphous Cs_2CO_3. In order to confirm this hypothesis, a TDXD experiment for Cs_2CO_3 (Aldrich, no. 44,190-2) was carried out in flowing air from room temperature to 550 °C. It was found that the lines displayed beyond 370 °C in the diffraction patterns shown in Fig. 6 were observed from 180 °C upwards. Good quality powder diffraction data for this phase were collected *in situ* at 200 °C. The corresponding pattern is shown in Fig. 7, as well as one of the patterns obtained from the TDXD plot, which shows both crystalline Y_2O_3 and Cs_2CO_3. The indexing of the pattern of this high-temperature variety of Cs_2CO_3 gave an orthorhombic solution, with the unit cell parameters $a=10.349(2)$, $b=8.269(1)$, $c=6.153(1)$ Å, $V=527.0$ Å^3 [$M_{20}=63$, $F_{30}=68(0.011,42)$]. The conditions for non-extinction were consistent with the space groups *Pnma* and $Pna2_1$. From this encouraging powder pattern indexing result with high figures of merit, it is reasonable to consider crystal structure determination from powder data. As seen on the TDXD plot (Fig. 6), new lines appear at room temperature, in addition to those of Y_2O_3, when the sample is cooled down. It has been shown that these lines are attributed to a polymorphic modification of Cs_2CO_3 observed at *ca.* 100 °C. Nevertheless, a thorough study of the thermal properties of caesium carbonate is in progress and will be reported elsewhere.

The successive stages of the thermal decomposition of $Y(H_2O)Cs(C_2O_4)_2$ under flowing nitrogen can be summarised as follows:

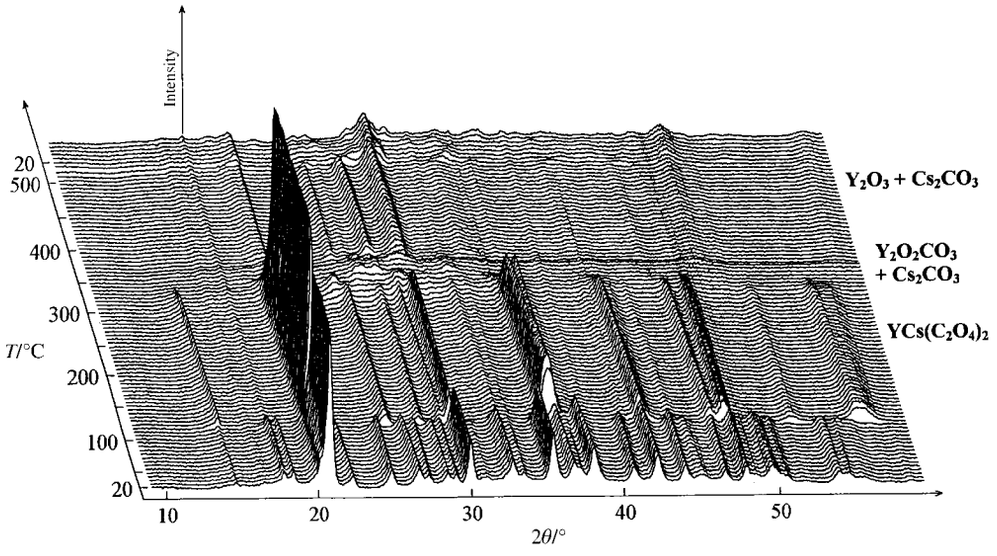

Fig. 6 TDXD plot for $Y(H_2O)Cs(C_2O_4)_2$ under nitrogen (heating rate 5 °C h^{-1}, counting time 75 min per pattern).

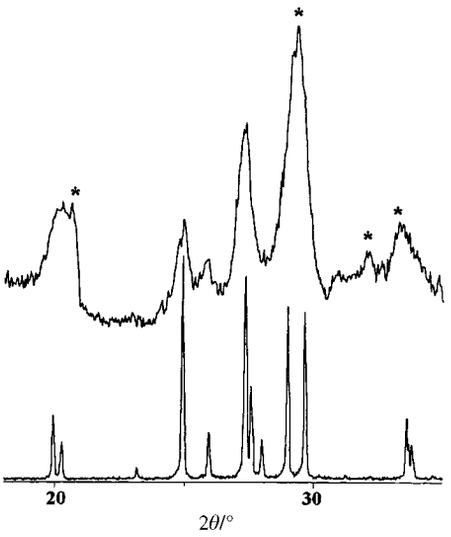

Fig. 7 X-Ray powder diffraction patterns of the high-temperature modification of Cs_2CO_3 (bottom) and the decomposition products of $Y(H_2O)Cs(C_2O_4)_2$ as revealed by TDXD at 450 °C (top). The asterisks indicate the diffraction lines of Y_2O_3.

$$Y(H_2O)Cs(C_2O_4)_2{\cdot}0.5H_2O \rightarrow Y(H_2O)Cs(C_2O_4)_2 + 0.5H_2O \quad (20\text{–}107\ ^\circ C)$$

$$Y(H_2O)Cs(C_2O_4)_2 \rightarrow YCs(C_2O_4)_2 + H_2O \quad (122\text{–}134\ ^\circ C)$$

$$YCs(C_2O_4)_2 \rightarrow 0.5Y_2O_2CO_3 + 0.5Cs_2CO_3 + CO_2 + 2CO \quad (270\text{–}335\ ^\circ C)$$

$$0.5Y_2O_2CO_3 \rightarrow 0.5Y_2O_3 + 0.5CO_2 \quad (335\text{–}370\ ^\circ C)$$

Conclusion

The present work forms part of the systematic study of the series of mixed oxalates with the general formula $LnM(C_2O_4)_2{\cdot}nH_2O$, where Ln stands for La or Y and M is a monovalent cation. The crystal structures of the mixed Y–NH_4, Y–Cs, Y–Na, La–NH_4 and La–K oxalates are two-dimensional with monovalent cations and water molecules lying between the layers.[3,9,18] Some of these phases present interesting cation exchange properties.[8] Roméro *et al.*[6] reported the crystal structure of $La(H_2O)Li(C_2O_4)_2{\cdot}H_2O$, which exhibits a three-dimensional network with one structurally-bonded water molecule. $YK(C_2O_4)_2{\cdot}4H_2O$ exhibits a three-dimensional porous framework in which the zeolitic water molecules are located in tunnels.[7] Further investigations are then needed to shed light on the rôle of the cations in the structure-type of these phases and in the dynamic properties described in the literature. Indeed, the preparation of new mixed oxalates containing rare earth elements and monovalent cations, such as Rb or Ag, could be helpful for understanding the crystal chemistry of this series.

Acknowledgements

Professor M. Louër is acknowledged for valuable discussions and Mr G. Marsolier for his technical assistance in powder data collection.

References

1 J. Sterba-Böhm and A. Pisaricek, *Collect. Czech. Chem. Commun.*, 1930, **2**, 244.
2 M. F. Barrett, T. R. R. McDonald and N. E. Topp, *J. Inorg. Nucl. Chem.*, 1964, **26**, 931.
3 T. R. R. McDonald and J. M. Spink, *Acta Crystallogr.*, 1967, **23**, 944.
4 E. G. Davitashvili, M. E. Modebadze and N. G. Sheliya, *Russ. J. Inorg. Chem.*, 1971, **16**, 349.
5 O. Gencova and J. Siftar, *J. Therm. Anal.*, 1995, **44**, 1171.
6 S. Roméro, A. Mosset and J. C. Trombe, *Eur. J. Solid State Inorg. Chem.*, 1995, **32**, 1053.
7 T. Bataille, J.-P. Auffrédic and D. Louër, *Chem. Mater.*, 1999, **11**, 1559.
8 V. Crespi Caramella, L. Maggi and M. T. Valentini Ganzerli, *Appl. Radiat. Isot.*, 1999, **51**, 353.
9 T. Bataille, M. Louër, J.-P. Auffrédic and D. Louër, *J. Solid State Chem.*, 2000, **150**, 81.
10 D. Louër and J. I. Langford, *J. Appl. Crystallogr.*, 1988, **21**, 430.
11 H. E. Swansson, M. C. Morris, E. H. Evans and L. Ulmer, in *National Bureau of Standards (USA) Monograph 25, Sect. 3*, National Bureau of Standards, Washington, DC, 1964, p. 1.
12 A. Boultif and D. Louër, *J. Appl. Crystallogr.*, 1991, **24**, 987.
13 J. Rodriguez-Carvajal, in *Collected Abstracts of Powder Diffraction Meeting*, Toulouse, France, 1990, p. 127.
14 J. Rodriguez-Carvajal and T. Roisnel, in *Commission on Powder Diffraction*, International Union of Crystallography, Newsletter no. 20, 1998, p. 35.
15 International Centre for Diffraction Data, Newton Square, PA, USA.
16 J.-F. Bérar and G. Baldinozzi, *J. Appl. Crystallogr.*, 1993, **26**, 128.
17 L. B. McCusker, R. B. Von Dreele, D. E. Cox, D. Louër and P. Scardi, *J. Appl. Crystallogr.*, 1999, **32**, 36.
18 T. Bataille and D. Louër, *Acta Crystallogr., Sect. C*, 1999, **55**, 1760.
19 I. D. Brown, *J. Appl. Crystallogr.*, 1996, **29**, 479.
20 V. Picard, PhD Thesis, Université de Bourgogne, 1993.